

# Cosmic-Ray Heating of Molecular Gas in the Nuclear Disk: Low Star Formation Efficiency

F. Yusef-Zadeh<sup>1</sup>, M. Wardle<sup>2</sup>, S. Roy<sup>3</sup>

## ABSTRACT

Understanding the processes occurring in the nuclear disk of our Galaxy is interesting in its own right, as part of the Milky Way Galaxy, but also because it is the closest galactic nucleus. It has been more than two decades since it was recognized that the general phenomenon of higher gas temperature in the inner few hundred parsecs by comparison with local clouds in the disk of the Galaxy. This is one of the least understood characteristics of giant molecular clouds having a much higher gas temperature than dust temperature in the inner few degrees of the Galactic center. We propose that an enhanced flux of cosmic-ray electrons, as evidenced recently by a number of studies, are responsible for directly heating the gas clouds in the nuclear disk, elevating the temperature of molecular gas ( $\sim 75\text{K}$ ) above the dust temperature ( $\sim 20\text{K}$ ). In addition we report the detection of nonthermal radio emission from Sgr B2-F based on low-frequency GMRT and VLA observations. The higher ionization fraction and thermal energy due to the impact of nonthermal electrons in star forming sites have important implications in slowing down star formation in the nuclear disk of our galaxy and nuclei of galaxies.

*Subject headings:* Galaxy: center - clouds - ISM: general - ISM - radio continuum - cosmic rays - stars: formation

---

<sup>1</sup>Department of Physics and Astronomy, Northwestern University, Evanston, IL 60208 (zadeh@northwestern.edu)

<sup>2</sup>Department of Physics, Macquarie University, Sydney NSW 2109, Australia (wardle@physics.mq.edu.au)

<sup>3</sup>Astron, P.O. Box 2, 7990 AA, Dwingeloo, The Netherlands (roy@astron.nl)

## 1. Introduction

The nuclear disk of our Galaxy has been studied extensively in molecular lines at millimeter wavelengths. Multi-transition ammonia observations have probed the temperature of gas (Güsten, Walmsley and Pauls 1981; Morris et al. 1983; Güsten et al. 1985; Hüttemeister et al. 1993), which was measured to be in the range of 50–120 K and was found to be uniformly high throughout the inner 500 pcs of the Galaxy. A high spatial resolution study of 36 clouds between  $l=-1^\circ$  and  $3^\circ$  (Hüttemeister et al. 1993) found a two-temperature distribution, warm low-density gas ( $T_{kin} \sim 200$  K,  $n(\text{H}_2) \sim 10^3 \text{ cm}^{-3}$ ) and cool dense cores ( $T_{kin} \sim 25$  K,  $n(\text{H}_2) \sim 10^5 \text{ cm}^{-3}$ ). In another study, ISO observations of rotational transitions of  $\text{H}_2$  found predominantly warm molecular gas with  $T \sim 150$  K toward 16 Galactic center molecular clouds with  $\text{H}_2$  column densities of  $\sim 1 - 2 \times 10^{22} \text{ cm}^{-2}$  (Rodríguez-Fernández et al. 2001). A recent absorption line study of the metastable (3,3) rotational level of  $\text{H}_3^+$  suggests that there is a large quantity of warm ( $T \sim 250$  K) and diffuse ( $n(\text{H}_2) \sim 100 \text{ cm}^{-3}$ ) gas distributed in the central few hundred pcs of the Galaxy (Oka et al. 2005).

Molecular gas with  $T \gtrsim 100$  K in the Galactic disk is heated by collisions with grains that have been warmed by hot stars in star forming regions. Thus, regions of high kinetic temperatures inferred in  $\text{NH}_3$  observations of star forming regions is strongly correlated with high dust temperature of clouds that accompany IR sources. However, the high gas temperature in GMCs in the nuclear disk (Lis et al. 2001) is inconsistent with the dust temperature 18–22 K inferred toward the inner  $2^\circ \times 1^\circ$  of the Galaxy from SCUBA 850 and 450  $\mu\text{m}$  and IRAS observations (Cox & Laureijs 1989; Pierce-Price et al. 2000).

A global heating mechanism is needed to explain the significantly higher gas temperature than dust temperature in a large fraction of gas and dust clouds in the nuclear disk. With the exception of Sgr B2, the lack of embedded sources able to provide significant heating is supported by the paucity of 6.7 MHz methanol sources in this region (Caswell 1996). High ionization by a large flux of cosmic rays heating Galactic center molecular clouds has been suggested by a number of authors (Güsten et al. 1981; Hüttemeister et al. 1993). Alternative suggestions such as cloud-collisions or global fast shocks have also been made but there is no clear observational evidence to support these hypotheses (Martin-Pintado et al. 1997; Lis et al. 2001). Here, we describe several recent studies indicating an excess cosmic ray flux in the central region of the Galaxy and revisit the cosmic ray heating scenario initially proposed by Güsten et al. (1981). We also report the detection of nonthermal radio emission from the massive star forming region Sgr B2 followed by the implications of cosmic ray interaction with molecular clouds. In particular, the consequences of such interaction is discussed in the context of star formation in the Galactic center region.

## 2. Evidence for Enhanced Cosmic Ray Flux

Our interest in reconsidering the global heating of molecular clouds by cosmic rays in the central 500 pcs stem from three different studies which infer enhanced cosmic rays there. First, the fluorescent 6.4 keV  $K\alpha$  iron line emission from the G0.11–0.08 molecular cloud, which lies  $\sim 15$  pcs in projection from the Galactic center (Tsuboi et al. 1997; Oka et al. 2001), is accounted for by the impact of low-energy cosmic ray electrons (Yusef-Zadeh, Law & Wardle 2002). The energy density over the  $10^6 M_\odot$  cloud was estimated to be  $1\text{--}2 \text{ eV cm}^{-3}$ , increasing to  $150 \text{ eV cm}^{-3}$  at the edge of the cloud where there it interacts with a nonthermal radio filament. The required energy density of cosmic rays at the edge of the cloud increases to  $\sim 250 \text{ eV cm}^{-3}$  if the molecular mass of G0.11–0.08 is  $6 \times 10^5 M_\odot$  (Handa et al. 2006). This idea was also applied to other prominent Galactic center molecular clouds from which diffuse 6.4 keV line emission is detected (Yusef-Zadeh et al. 2007a). The energy density of the cosmic rays required to explain the observed X-ray emission from the clouds in the inner  $2^\circ \times 0.5^\circ$  of the Galaxy ranges between 20 and  $10^3 \text{ eV cm}^{-3}$ . A cosmic-ray energy density of  $0.2 \text{ eV cm}^{-3}$  is required to explain the Galactic ridge X-ray emission (Valinia et al. 2000). The inferred ionization rates of the Galactic center clouds based on the 6.4 keV line measurements range between  $2 \times 10^{-14}$  and  $5 \times 10^{-13} \text{ s}^{-1} \text{ H}^{-1}$  (Yusef-Zadeh et al. 2002, 2007a).

Second, strong  $\text{H}_3^+$  absorption along several lines of sight towards the Galactic center has been reported by Oka et al. (2005), who inferred that the ionization rate in this unique environment ranges between  $2\text{--}7 \times 10^{-15} \text{ s}^{-1}$ . Furthermore, an  $\text{H}_3\text{O}^+$  study toward Sgr B2, one of the densest clouds in the Galaxy, inferred also an ionization rate of  $\sim 4 \times 10^{-16} \text{ s}^{-1}$  (van der Tak et al. 2006).

Third, the detection of low frequency 74 MHz radio emission from the central disk of the Galaxy indicates enhanced cosmic rays from the central degree of the Galaxy. LaRosa et al. (2005) estimate that the cosmic ray electron density of the central  $1.5 \times 0.5$  degrees is  $\sim 7.2 \text{ eV cm}^{-3}$ , about 15 times higher than that in the local ISM (Webber 1998). In addition, detailed spectral index measurements of extended radio sources show that  $85 \pm 4\%$  of 6 cm continuum emission corresponding to a flux density of  $841 \pm 44 \text{ Jy}$  from the inner  $\sim 2.5^\circ \times 1^\circ$  of the Galaxy is nonthermal (Law 2007).

## 3. GMRT and VLA Radio Continuum Analysis

Motivated by the strong detection of 6.4 keV line emission from Sgr B2, we searched for evidence of nonthermal continuum emission from this cloud. To examine the picture of

cosmic-rays impacting molecular gas in Sgr B2, observations were conducted on March 14, 2003 using the Giant Meterwave Radio Telescope (GMRT) at 255 and 583 MHz with an effective bandwidth of 6 MHz using the default spectral line mode of the correlator. The field center was set at  $\alpha, \delta(J2000) = 17^h46^m00^s, -28^d57'00''$ . 3C48 was used as primary flux density calibrator, and 1830-36 was used as secondary calibrator. The data were processed using standard programs in AIPS. After calibration and editing of the 255 MHz data, a pseudo-continuum database of 9 frequency channels was made from the central 5.6 MHz of the observed 6 MHz band. Images of the fields were formed after the application of phase self-calibration.

In addition, we used archival data taken with the Very Large Array (VLA) of the National Radio Astronomy Observatory<sup>1</sup> at 1.4 GHz and 327 MHz. The data reduction is described in Yusef-Zadeh, Hewitt, & Cotton (2004) and Nord et al. (2004), respectively.

Figure 1a shows contours of 255 MHz radio continuum emission superimposed on a grayscale image of Sgr B2 at 327 MHz. The peak emission at 327 MHz centered at  $\alpha, \delta(J2000) = 17^h47^m201.6^s, -28^d23'03.63''$  coincides with the position of the brightest cluster of 20 ultracompact HII regions known as the F cluster in Sgr B2 Main (DePree et al. 1998). To determine the flux density of this source at 1.4 GHz and 255 MHz, we used Gaussian-fitted fluxes from background subtracted images. Figure 1b shows the spectrum of the emission based on images convolved to  $22.5'' \times 16.8''$  resolution. The high frequency emission from Sgr B2 is due to bright, compact and optically thick HII regions whose flux densities should drop with decreasing frequencies. Increased free-free absorption by foreground material is responsible for the drop in the flux density at low frequencies (see below).

Despite the complexity of bright radio emission from Sgr B2, there is evidence for nonthermal emission at low frequencies. First, it is clear that the isolated emission from the F cluster dominates this complex region at low frequencies but has similar surface brightness to Sgr B2 North at high frequencies. The 1490 MHz images of the Sgr B2 M and N show peak flux densities of  $\sim 1.1$  Jy within a beam size of  $10'' \times 10''$  (Yusef-Zadeh, Hewitt and Cotton 2004).

Second, the spectral index  $\alpha$ , where  $F_\nu \propto \nu^\alpha$ , between 255 and 327 MHz is estimated to be  $1.28 \pm 0.4$  whereas  $\alpha$  is  $2.35 \pm 0.30$  between 1490 and 583 MHz. A flatter spectral index suggests a steep spectrum emission is contributing to the flux of Sgr B2 at low frequencies. This inference is strengthened by the fact that the measured flux density at 255 MHz would be higher had the effect of foreground free-free absorption been accounted for. Assuming

---

<sup>1</sup>The National Radio Astronomy Observatory is a facility of the National Science Foundation, operated under a cooperative agreement by Associated Universities, Inc.

that the free-free absorption optical depth is  $\sim 1$  at 150 MHz (Roy & Rao 2006), is  $\propto \lambda^{2.1}$ , and is the same toward both Sgr B2 and the Sgr A complex, then  $\tau \sim 0.33$  and  $0.19$  at 255 and 327 MHz, respectively. The unabsorbed flux density of Sgr B2 region would then imply  $\alpha = 0.81 \pm 0.4$  between 255 and 327 MHz. This shows that the radio spectrum becomes flatter at lower frequencies, as shown in Figure 1b. Furthermore, if we extrapolate the flux density at 1490 MHz to 255 MHz with a  $\sim 2.3$  spectral index, the flux density is expected to be  $\sim 160$  mJy which is lower than the unabsorbed flux density of 242 mJy at 255 MHz. The difference between the measured and estimated flux densities at 255 MHz is 82 mJy. Assuming that the thermal and nonthermal components are distinct, the nonthermal component at 255 MHz is estimated to be 82 mJy.

Third, two studies of nonthermal emission from Sgr B2 provide further evidence for cosmic rays associated with Sgr B2 (Hollis et al. 2007; Crocker et al. 2007). Detailed GBT observations of Sgr B2 report a flux  $\sim 4.6$  Jy at 44 GHz with  $\alpha = -0.7$  (Hollis et al. 2007). The nonthermal radio flux needed to explain the 6.4 keV line emission from Sgr B2 is 18 Jy at 327 MHz (Yusef-Zadeh et al. 2007a). Thus, the observed nonthermal flux measured with GBT is more than enough to account for the origin of the observed 6.4 keV line emission from Sgr B2. We believe a fraction of the observed nonthermal emission from Sgr B2 is localized with the Sgr B2 F cluster and the rest is diffuse over a larger extent associated with Sgr B2.

Finally, radio continuum and radio recombination line studies indicate an unusually high electron temperature, high brightness temperature, rising spectral index and an anomalously low helium abundance at the position of the F cluster in Sgr B2 (Mehringer et al. 1995; DePree et al. 1998). A nonthermal contribution to the continuum emission could be responsible for the low line-to-continuum ratio, and thus the inferred high brightness temperature as well as the abundance of atomic and molecular species affected by the bombardment of cosmic ray particles. A more detailed account will be given elsewhere.

To estimate the energy density of electrons we adopt a typical nonthermal flux of 80 mJy at 255 MHz in a  $22.''5 \times 16.''8$  beam, with a  $\nu^{-0.7}$  spectrum. The relativistic electrons responsible for the emission must have an  $E^{-2.4}$  energy spectrum, and we suppose that this extends down to 1 MeV. Their energy density is  $\sim 3 \text{ eV cm}^{-3}$  for  $B = 1 \text{ mG}$  or  $\sim 150 \text{ eV cm}^{-3}$  for  $B = 0.1 \text{ mG}$ . The corresponding ionization rate can be estimated by noting that in the MeV range the stopping power of the ISM is about  $3.5 \text{ MeV g}^{-1} \text{ cm}^2$  (ICRU 1984), and that on average one ionization occurs for each 40.1 eV deposited into the gas (Dalgarno, Yan & Liu 1999). This yields an ionization rate  $\sim 2 \times 10^{-14} \text{ s}^{-1} \text{ H}^{-1}$ . The energy density and ionization rate are reduced by a factor  $\sim 25$  if the electron spectrum only extends down to 10 MeV instead of 1 MeV.

## 4. Discussion

### 4.1. Effects of Enhanced Cosmic Ray Fluxes in Star Forming Regions

High cosmic-ray fluxes in molecular clouds affect star formation by heating the gas and increasing its ionization fraction. Higher cloud temperatures increase the Jeans mass, potentially changing the IMF, while high ionization increases magnetic coupling to the cloud material, reducing ambipolar diffusion and increasing the time taken for gravitationally unstable cores to contract to the point that they overwhelm their magnetic support.

The heating associated with cosmic ray ionizations can be estimated as follows. Each ionization of a hydrogen molecule is associated on average with 40.1 eV energy loss by electrons, of which 11% ends up as heat (e.g. Dalgarno et al. 1999). In addition another 8 eV appears as heat when  $\text{H}_3^+$  recombines (e.g. Maloney, Hollenbach & Tielens 1996). Thus, each ionization of a hydrogen molecule is associated with the deposition of 12.4 eV of heat into the gas. As the ionization rate per hydrogen *nucleus* is half the  $\text{H}_2$  ionization rate  $\zeta_{\text{H}}$ , the heating rate per hydrogen nucleus  $\Gamma/n_{\text{H}}$  is  $\approx 25 \text{ eV} \times \zeta_{\text{H}}$ , or

$$\Gamma/n_{\text{H}} = 4.0 \times 10^{-26} \left( \frac{\zeta_{\text{H}}}{10^{-15} \text{ s}^{-1} \text{ H}^{-1}} \right) \text{ erg s}^{-1} \text{ H}^{-1} \quad (1)$$

As pointed out by Güsten et al. (1981), an ionization rate  $\zeta_{\text{H}} \sim 1 \times 10^{-15} \text{ s}^{-1}$  is sufficient to explain the observed gas temperature of  $\sim 70 \text{ K}$ . Using the cooling rates calculated by Neufeld, Lepp & Melnick (1995) for  $n(\text{H}_2) = 5000 \text{ cm}^{-3}$  and  $N(\text{H}_2)/\Delta v = 10^{22} \text{ cm}^{-2} \text{ km}^{-1} \text{ s}$ , the equilibrium temperatures are approximately 60, 130 and 280 K for  $\zeta_{\text{H}} = 10^{-15}$ ,  $10^{-14}$  and  $10^{-13} \text{ s}^{-1} \text{ H}^{-1}$  respectively.

The Jeans mass can be estimated by equating the free-fall time of a uniform cloud core of density  $\rho$  and radius  $R$ , i.e.  $t_{\text{ff}} = 1/\sqrt{G\rho}$ , to the sound crossing time  $R/c_s$ , yielding

$$M_J \approx 11 \left( \frac{T}{75 \text{ K}} \right)^{3/2} \left( \frac{n_{\text{H}}}{10^6 \text{ cm}^{-3}} \right)^{-1/2} M_{\odot} \quad (2)$$

Collapse of this Jeans-unstable core is halted by the cloud's magnetic field if the mass-to-flux ratio is less than the critical value  $1/\sqrt{4\pi G}$ , ie. if  $B \gtrsim 0.1 n_{\text{H}} / (10^6 \text{ cm}^{-3}) \text{ mG}$ . However the magnetic support is temporary because the cloud is weakly-ionized, and the predominant neutral species are able to drift towards the centre under the action of gravity while colliding with the ions and electrons that are tied to and supported by the near-static field lines. The neutral drift speed is determined by the balance between gravity and the drag due to collisions with the ions:

$$\frac{GM\rho}{R^2} \approx n_i < \sigma v > \rho v_d \quad (3)$$

where  $\langle \sigma v \rangle \approx 2 \times 10^{-9} \text{ cm}^{-3} \text{ s}^{-1}$  is the rate coefficient for ion-neutral momentum transfer. This yields a drift speed of a few hundredths of a kilometer per second. This drift increases the mass-to-flux ratio at the core’s centre on a time scale

$$t_{\text{AD}} = \frac{R}{v_d} \approx 0.8 \left( \frac{x_e}{10^{-8}} \right) \text{ Myr} \quad (4)$$

until it attains the critical value at which point dynamical collapse occurs on a few free-fall times. A more accurate calculation by Mouschovias (1987) reduces this estimate by a factor of two. The ambipolar diffusion timescale is of order a few Myr for the standard interstellar ionization rates but is directly proportional to the ionization fraction, or equivalently to the square root of the ionization rate. Thus the time scale to achieve a supercritical core becomes large if the ionization rate is increased a hundred-fold over standard values.<sup>2</sup>

Recent observations indicate that massive star formation has signatures similar to those seen in low-mass star formation: low star formation efficiency (Krumholz & Tan 2007), disc accretion (e.g. Cesaroni et al. 2005) and molecular outflows (e.g. Zhang et al. 2005). If the initial phases of high-mass star formation are analogous to low-mass star formation, then the formation of high mass stars should be affected by the increased cosmic-ray ionization rate. Due to the higher Jeans mass in the warm gas, more massive stars are expected to preferentially form in the nuclear disk. This scenario is consistent with recent observations of a number of unique and young massive stellar clusters with a top heavy IMF (Figer et al. 2004; Stolte et al. 2005; Nayakshin & Sunyaev 2005).

In this environment, the strong tidal shear will allow only the densest clouds to survive. Survival against shear requires that the gravitational frequency of the cloud,  $\sqrt{G\rho}$ , must exceed the orbital frequency around the Galactic Centre,  $v/R$ . Adopting a galactocentric distance  $R = 100 \text{ pc}$  and an orbital speed  $v = 150 \text{ km/s}$ , we find that clouds are tidally stable only if  $n_{\text{H}} > 1.5 \times 10^4 \text{ cm}^{-3}$ .

## 4.2. Implications & Conclusions

The mass of the molecular nuclear disk is estimated to be  $2 - 6 \times 10^7 M_{\odot}$  (Oka et al. 1998; Pierce-Price et al. 2000) with typical gas temperature  $\sim 70 \text{ K}$ , so the cosmic ray heating in this region totals  $\sim 2 - 6 \times 10^{37} \text{ erg s}^{-1}$ . The total cosmic-ray energy losses are five times higher, i.e.  $\sim 1 - 3 \times 10^{38} \text{ erg s}^{-1}$ . Assuming that  $\sim 10^{50} \text{ ergs}$  ( 10% of the energy of a

---

<sup>2</sup>see Le Petit et al. (2004) and references therein for recent determinations of the ionization rate in diffuse clouds

typical supernova) goes into particles and the magnetic field (Duric et al. 1995), it leads to one supernova per  $10^4$  years. Given the high density molecular gas in the nuclear disk, a SNR lifetime of  $\sim 2 \times 10^4$  yr implies a few SNRs in the nuclear disk, comparable to the number of known SNRs (Gray 1994). The uniformity of the dense molecular gas distributed in the nuclear disk is inferred from the fact that  $\sim 60\%$  of all known remnants in this region interact with molecular gas versus a value of  $10\%$  in the Galactic disk (Yusef-Zadeh et al. 2007b). Assuming a Miller-Scalo IMF, the above estimate of the SN rate implies a star formation rate ( $> 5 M_\odot$ ) of  $\sim 2.5 \times 10^{-3} M_\odot \text{yr}^{-1}$  (e.g., Condon 1992). Given that  $\sim 5\%$  of the molecular gas in the Galaxy resides in the nuclear disk, the estimated star formation activity per unit mass, as traced by SN rate, is two orders of magnitude lower than that in the Galactic disk. Thus, star formation is fairly inefficient in this region of the Galaxy. Fatuzzo, Adams & Melia (2006) also suggest that the increased ionization resulting from the interaction of supernova remnants with molecular clouds acts to suppress star formation.

Increased ionization due to enhanced cosmic rays is responsible for the lower efficiency of star formation in the Galactic nuclear disk than in the Galactic disk. Sgr B2 is the best example of current massive star formation in the nuclear disk, but even there the star formation per unit mass in Sgr B2 is an order of magnitude lower than that in W49 and W51, massive star forming regions in the main spiral arms of the Galaxy (Gordon et al. 1993). All other massive clouds in the nuclear disk show even lower efficiency of star formation than in Sgr B2. For example, the giant molecular cloud G0.25+0.01 has a star formation efficiency of  $0.1\%$ , roughly 30 times less than that in the disk of the Galaxy (Lis et al. 2001). The lack of numerous  $\text{H}_2\text{O}$  and methanol masers usually associated with early phases of star formation, especially in light of the large reservoir of warm and dense molecular clouds in this region also indicates that the overall star formation rate in the molecular nuclear disk is generally low.

In conclusion, we have presented the evidence of cosmic rays in Sgr B2, arguably, the most massive star forming regions in the Galaxy. We have also outlined a simple picture of the heating of molecular gas by cosmic rays and its consequent high ionization fraction can delay the formation of stars, suppress the formation of low-mass stars in a high pressure environment. The impact of the relativistic component of the ISM with molecular clouds has important implications for the mode of star formation and also the type of energetic activity found in nuclei of galaxies. A recent CO (7–6) line observations of NGC 253 (Bradford et al. 2003) also supports a picture in which cosmic rays are responsible for heating the molecular gas in the nucleus of this starburst galaxy.

Acknowledgments: We thank the referee and the editor, John Scalo, for useful comments.



## REFERENCES

- Bradford, C. M., Nikola, T., Stacey, G. J., Bolatto, A. D., Jackson, J. M., Savage, M. L., Davidson, J. A. & Higdon, S. J. 2003, *ApJ*, 568, 891
- Caswell, J. L. 1996, *MNRAS*, 283, 606
- Cesaroni, R., Neri, R., Olmi, L., Testi, L., Walmsley, C. M. & Hofner, P. 2005, *A&A*, 434, 1039
- Condon, J. J. 1992, *ARA&A*, 30, 575
- Cox, P. & Laurejs, R. 1989, *IAU Symp.* 136 on the Center of the Galaxy, ed: M. Morris, 121
- Crocker, R. M. et al. 2007, *ApJ*, in press, (arXiv:astro-ph/0702045)
- DePree, C. G., Goss, W. M. & Gaume, R. A. 1998, *ApJ*, 500, 847
- Duric, N., Gordon, S. M., Goss, W. M., Viallefond, F. & Lacey, C. 1995, *ApJ*, 445, 173
- Fatuzzo, M. Adams & Melia, F. 2006, *ApJ*, 653, L49
- Figer, D. F. et al. 2004, *ApJ*, 601, 319
- Goldsmith, P. F. & Langer, W. D. 1978, *ApJ*, 222, 881
- Gordon, M. A. et al. 1993; *A&A*, 280, 208
- Gray, A. D. 1994, *MNRAS*, 270, 861
- Güsten, R., Walmsley, C.M., Ungerechts, H. & Churchwell, E. 1985, *A&A*, 142, 381
- Güsten, R., Walmsley, C.M. & Pauls, T. 1981, *A&A*, 103, 197
- Handa, T., Sakano, M., Naito, S., Hiramatsu, M. & Tsuboi, M. 2006, *ApJ*, 636, 261
- Hollis, J. M., Jewell, P. R., Remijan, J. & Lovas, F. J. 2007, *ApJ*, 660, L125
- Hüttemeister, S., Wilson, T.L., Banina, T.M., Martin-Pintado, J. 1993, *A&A*, 280, 255
- ICRU 1984, Stopping Powers for Electrons and Positrons ( ICRU Rept. 37; Bethesda: ICRU)
- Krumholz, M. R. & Tan, J. C. 2007, *ApJ*, 654, 304
- LaRosa, T. N., Brogan, C. L., Shore, S. N., Lazio, T. J., Kassim, N. E. & Nord, M. 2005, *ApJ*, 626, L23

- Law, C. 2007, PhD thesis, Northwestern University
- Le Petit, F., Roueff, E. & Herbst, E. 2004, *A&A*, 417, 993
- Lis, D. C., Serabyn, E., Zylka, R. & Li, Y. 2001, *ApJ*, 550, 761
- Maloney, P. R., Hollenbach, D. J. & Tielens, A. G. G. M. 1996,
- Martin-Pintado, J., de Vicete, P., Fuente, A. & Planesas, P. 1997, *ApJ*, 482, L45.
- McKee, C. F. & Tan, J. C. 2004, *ApJ*, 585, 850
- Mehring, D. M., DePree, C. G. , Gaume, R. A., Goss, W. M. & Claussen, M. J. 1995, *ApJ*, 442, L29
- Morris, M., Polish, N., Zuckerman, B. & Kaifu, N. 1983, *AJ*, 88, 1228
- Mouschovias, T. C. 1987, in *Physical Processes in Interstellar Clouds*, ed. G. E. Morfill & M. Scholer (Dordrecht: Reidel), 453
- Nayakshin, S. & Sunyaev, R. 2005, *MNRAS*, 364, L23
- Neufeld, D. A., Lepp, S. & Melnick, G. J. 1995, *ApJ Supp*, 100, 132
- Nord, M.E., Lazio, T.J.W., Kassim, N.E., Hyman, S.J., LaRosa, T.N., Brogan, C.L. & Duric, N., 2004, *AJ*, 128, 1646
- Oka, T., Hasegawa, T., Sato, F., Tsuboi, M. & Miyazaki, A. 2001, *PASJ*, 53, 779
- Oka, T., Geballe, T. R., Gioto, M., Usuda, T., McCall, B. J. 2005, *ApJ*, 632, 882
- Pierce-Price, D., Richer, J. S., Greaves, J. S., Holland, W. S., Jennes, T. 2000, *ApJ*, 545, L121
- Rodriguez-Fernandez, N. J., Martin-Pintado, J., Fuente, A., de Vicente, P., Wilson, T.L. & Hüttemeister, S. 2001, *A&A*, 365, 174
- Roy, S. & Rao, A. 2006, *Journal of Physics: Conference Series*, 54, 156
- Serabyn, E. & Güsten, R. 1986, *A&A*, 161, 334
- Stolte, A., Brandner, W., Grebel, E. K., Lenzen, R., Lagrange, A.-M., 2005, *ApJ*, 628, L113
- Tsuboi, M., M., Ukita, N., & Handa, T. 1997, *ApJ*, 481, 263
- Valinia, A., Tatischeff, V., Arnauld, K., Ebisawa, K. & Ramaty, R. 2000, *ApJ*, 543, 733

- van der Tak, F.F.S., Belloche, A., Schilke, P., Güsten, R., Philipp, S., Comito, et al. 2006, A&A, in press
- Webber, W. R. 1998, ApJ, 506, 329
- Yusef-Zadeh, F. et al. 2007b, in Astrophysical Masers and Their Environments, IAU Symp. 242, eds: J. Chapman & W. Baan, in press (arXiv:astro-ph/0705.3001)
- Yusef-Zadeh, F., Hewitt, J. W. & Cotton, W. 2004, ApJS, 155, 421
- Yusef-Zadeh, F., Law, C. & Wardle, M. 2002, ApJ, 568, L121
- Yusef-Zadeh, F., Nord, M., Wardle, M., Law, C., Lang, C. & Lazio, T. J. W. 2003, ApJ, 590, L103
- Yusef-Zadeh, F., Muno, M., Wardle, M. & Lis, D.C. 2007a, ApJ, 656, 847
- Zhang, Q., Hunter, T. R., Brand, J., Sridharan, T. K., Cesaroni, R., Molinari, S., Wang, J. & Kramer, M. 2005, ApJ, 625, 864

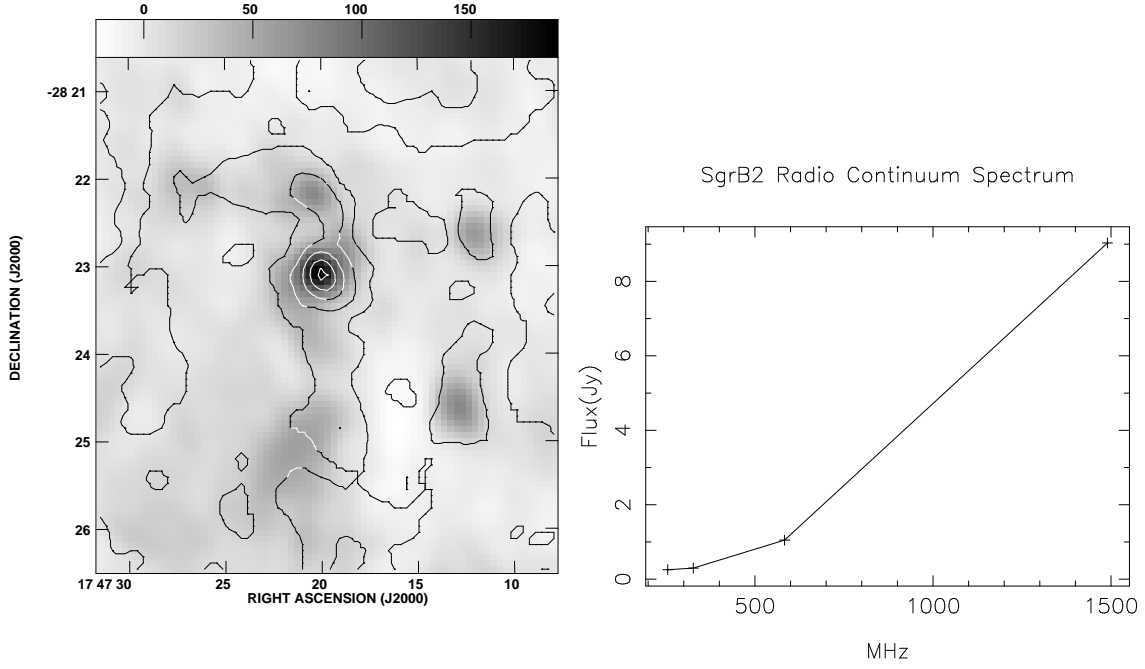


Fig. 1.— **(a) Left** Contours of 255 MHz emission at 30, 50, 70, 90, 120, 160, 200 mJy beam<sup>-1</sup> with spatial resolution of 22.5'' and 16.8'' (PA=19°) are superimposed on a grayscale image of the F source in Sgr B2 at 327 MHz (Nord et al. 2004). The peak position coincides with the cluster Sgr B2 F. The grayscale ranges between -20 and 188 mJy beam<sup>-1</sup>. The 255 MHz map has used UV data from 0.04 to 17 kλ to bring out extended features. The RMS noise is about 10 mJy beam<sup>-1</sup>. The compact sources show a positional accuracy 3-4'' compared to higher frequency observations. **(b) Right** The spectrum of Sgr B2-F at 255, 327, 583 and 1490 MHz, corrected for free-free absorption due to foreground gas (see text). Crosses indicate 1σ error bars.